Complete wavefield imaging for lithology and fluid prediction in the Barents Sea

Grunde Rønholt, Øystein Korsmo, Sören Naumann, Stepan Marinets, PGS, Even Brenne, Muhammad Faheem Abbasi, Statoil*

Summary:

In the shallow water environment found in parts of the Barents Sea, conventional imaging struggles to successfully resolve the near surface. This is due to the lack of near offsets (angles) in typical marine seismic data, caused by the large minimum distance between the source and receivers. Here, we present a method that uses separated (up- and down-going) wavefields provided by dual-sensor streamer technology to construct images and image gathers that span a complete range of incidence angles. In this method, each receiver is also used as a virtual source, hence providing a dataset that has complete coverage of zero- and near-offsets everywhere under the seismic spread. In particular, this provides near-angles for shallow targets that are not sampled by primaries, enabling amplitude versus angle (AVA) analysis to be carried out. The AVA results can be used to derive a direct hydrocarbon indicator (DHI) that would otherwise be impossible to achieve using primaries alone.

Introduction:

A 5,600 km^2 seismic survey covering the Northern area of the former disputed zone between Norway and Russia (Figure 1) was acquired in the Barents Sea during the summer of 2014. An exacting weather window and aggressive deadlines meant that acquisition efficiency was the priority. Consequently, the vessel deployed 10 deep-towed (15m) dual-sensor streamers, 7km long and 75m apart. This relatively small streamer separation (compared to the more common 100m for exploration surveys) was intended to improve illumination of shallow targets. Indeed, throughout the Barents Sea, the main plays consist in shallow high amplitude events and/or flat spots. The high amplitude is a response to the combination of lithology and fluids. Low/high gas saturation as well as oil appear with a similar seismic response (Figure 2), which makes it hard to find a discriminating DHI.

Acquiring 3D towed-streamer marine seismic in shallow waters always involves a compromise between efficiency and near-surface sampling. The wider the spread (number of cables times cable separation), the larger the distance between sail lines, resulting in more efficient data gathering. However, this configuration can suffer from acquisition footprint due to the lack of small offsets recorded on the outer cables. This lack of near-offset data at the swath boundaries leaves shallow illumination holes, which limit our ability to pick velocities based on gather flatness, and prevent the use of AVO/AVA type studies.

Wapenaar et al. (2010) and Whitmore et al. (2010) showed that sea-surface reflections, which are captured in the down-going wave of multi-sensor streamer acquisitions, can be used as virtual sources and provide the near-surface information missing from primary reflections. This feature has been used as part of the complete wavefield imaging (CWI) workflow to unravel the shallow heterogeneities prevalent in the North Sea and obtain more accurate depth models (Rønholt et al., 2014). In the case of the Barents Sea, sea-surface reflections can provide a direct and improved image of shallow targets, along with full angle gathers and the potential for a more discriminating DHI.

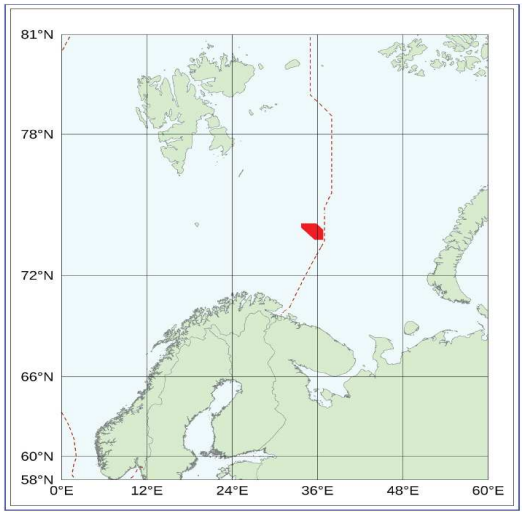

Figure 1: Study area in red – Barents Sea South East.

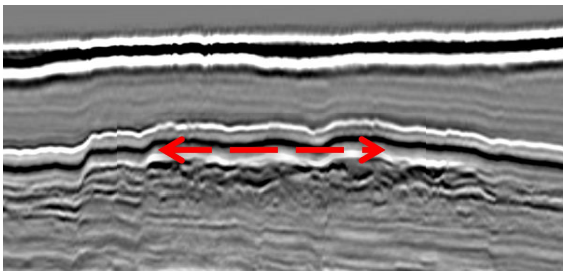

Figure 2: Amplitude brightening (white event below the red arrow) as seen in the BSSE data.

DOI http://dx.doi.org/10.1190/segam2015-5869968.1

Methodology:

In Complete Wavefield Imaging (CWI), the velocity model building workflow is made up of three main elements: wavelet shift tomography (Sherwood et al., 2014), full waveform inversion (FWI) and separated wavefield imaging (SWIM). The key to producing highly accurate velocity models lies in how these algorithms are combined into a workflow that mitigates any weakness that might exist in any one method alone (Rønholt et al., 2014).

Leveraging the good low frequency data recorded by dual-sensor streamers towed deep, FWI is producing high-resolution velocity updates from the seafloor down to depths where the refracted energy diminishes. Figure 3 illustrates that the refracted and other diving waves propagate through the shallow targets in this area of study.

The conventional depth migration with primaries backward extrapolates the upcoming data as receiver wavefield, and forward extrapolates a synthetic point source. In SWIM, after carrying out wavefield separation using a dual-sensor recording of the wavefield, we use the down-going wavefield as source and the up-going wavefield as receiver wavefield (Whitmore et al., 2010). This effectively turns each receiver into a virtual source, hence increasing the source sampling and coverage at the surface. The improved data coverage this provides helps mitigate acquisition footprint and provides enhanced angular illumination in the shallow sub-surface (Lu et al., 2014)

Because of the complexity of the up- and down-going wavefields' interaction, a deconvolution imaging condition is applied at the subsurface. This effectively reduces the cross-talk noise generated from unrelated correlation of up- and down-going wavefields. Angle gathers are generated from subsurface offset gathers after applying a radial trace transforms. The angle gathers obtained from imaging of multiples provide better illumination than the gathers obtained from primary reflection migrations (Lu et al., 2014).

Results:

The Barents Sea is known for its hard seafloor due to older, compacted sediments being exposed by uplift and erosion during the last ice age (Grogan et al., 1999). Locally, slightly slower Quaternary sediments are exposed. Highly compacted shales exhibit an extreme anisotropy regime with horizontal velocities as much as 35% higher than vertical velocities (Rønholt et al., 2008). A starting gradient velocity model with corresponding anisotropy parameters was established based on scanning and evaluation of modeled versus observed refractions, migrated reflection and multiple gather move-out. This was followed by velocity updates and anisotropy adjustments through the use of wavelet shift tomography. A long wavelength velocity model was achieved describing the refractions, primary reflections and sea-surface reflection data well. Iterative FWI was run in order to solve for gradually shorter wavelengths of velocity (Figure 4).

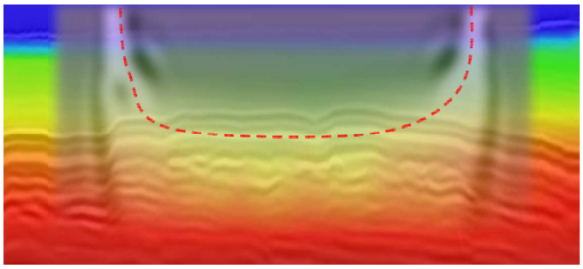

Figure 3: Seismic image of a shallow target structure with interval velocity model overlaid. An illustration of a forward modelled, 2-6Hz diving wave has been superimposed to the plot – where the white event (highlighted with a red, dashed line) represents the wave propagation. The source to receiver offset for the modelled wave is 6km and the depth shown is from 0 to 1.5km.

The velocity model after FWI was used to migrate both primary reflections and sea-surface reflections. The resulting angle gathers show significantly different illumination (Figure 5). The primary reflection gathers lack contributions to the near-angles due to the relatively large minimum offset acquired relative to target depth. At a depth of 600m the minimum angle varies from 15 to 20°. The sea-surface reflection gathers display a full angular coverage from 0 to 45°.

A comparison of the partial angle-stacks from the migration of sea-surface reflections is shown in Figure 6. For the selected line we observe both Class 2 (dimming at near angles) and Class 3 (no dimming) AVA anomalies. The area indicated by the red arrow exhibits a near to far slight, gradual increase in amplitude, while the area indicated by the blue arrow exhibits a much higher increase in amplitude from near to far angles. More analysis is required to correlate these two AVA behaviors with specific fluids and lithology content, but their clear differentiation bodes well for the definition of a discriminating DHI. Note that the primaries with their inherent limitation to far-angles cannot distinguish Class 2 from Class 3 AVA anomalies. A formal description of the various AVO classes can be found in Rutherford and Williams (1989).

DOI http://dx.doi.org/10.1190/segam2015-5869968.1

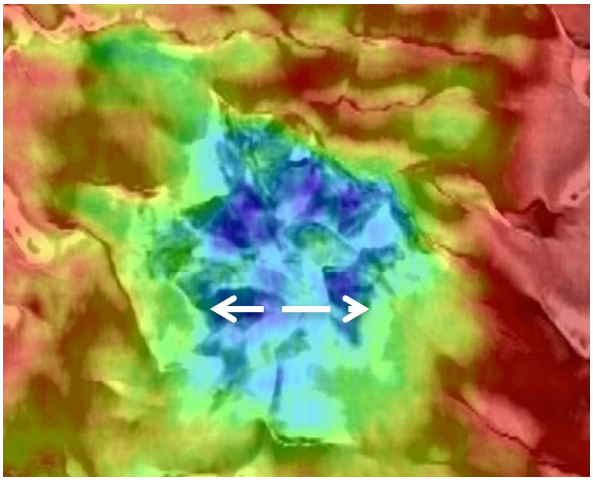

Figure 4: FWI velocity model overlaid on a seismic reflection image at 600m depth. Note the high level of detail at the faulted crest of the structure (blue colors) and co-located with the bright spots seen in the reflection image (same location as red arrow in figure 2).

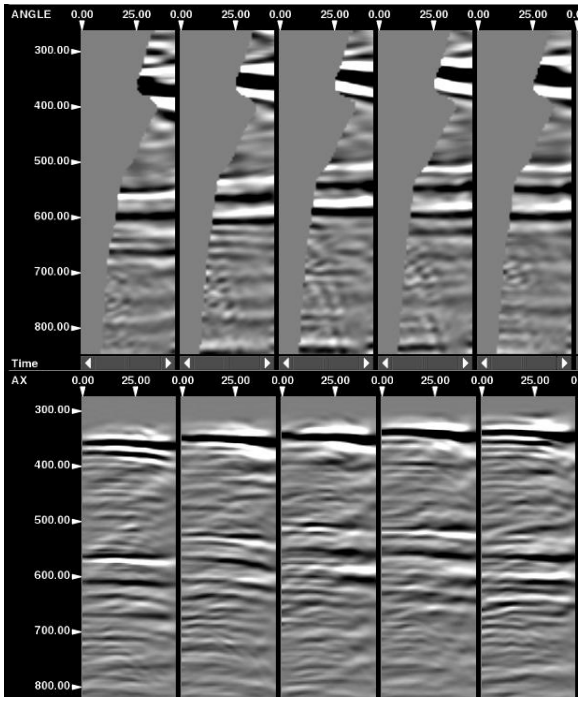

Figure 5: Angle gathers from migration of primary reflections (top) and sea-surface reflections (bottom). The five gathers are from the same relative location and the horizontal axis is angle in degrees, 0 to 45.

Conclusions:

Imaging shallow targets with primary reflection energy requires expensive and inefficient seismic acquisition to preserve a small enough near-offset throughout the survey. This is impractical in the Barents Sea where the weather window is very limited. Using sea-surface reflections for imaging circumvent this problem because multiples sample near-angles much better than primaries.

Dual-sensor streamers, in addition to increasing the weather window through deep-tow, provide enhanced low frequencies as well as up- and down-going wavefields. These features are used to determine a highly accurate shallow velocity model and provide a high resolution image of the shallow targets. Sea-surface reflections also provide fully populated angle gathers, which enable AVA analysis.

The shallow bright spots in the Barents Sea South East exhibit both Class 2 and Class 3 AVA behaviors. Although the correlation to specific fluids and lithology content remains to be done, the distinction is quite pronounced and appears to be discriminating. Such a DHI could not be obtained with primaries alone due to their deficiency in near-angles. Sea-surface reflections therefore provide unique insights for lithology and fluid prediction.

Acknowledgements:

We are very grateful to the group shoot partnership for allowing us to publish this work. The group shoot partners are Statoil, Shell, BP, Chevron, ConocoPhillips, ExxonMobil, E-ON, Det Norske, ENI, GdF Suez, Idemitsu, Lukoil Overseas, Lundin Norway, PGNiG, Repsol, Spike Exploration, Suncor, Wintershall, KUFPEC, INPEX, Total, OMV, Tullow Oil, RN Nordic, BG, DEA Norge and MOECO. We thank PGS for supporting this publication and Sverre Brandsberg-Dahl, Nizar Chemingui, Alejandro Valenciano, Dan Whitmore, Volker Dirks, Guillaume Cambois and Shaoping Lu for invaluable input to this study.

DOI http://dx.doi.org/10.1190/segam2015-5869968.1

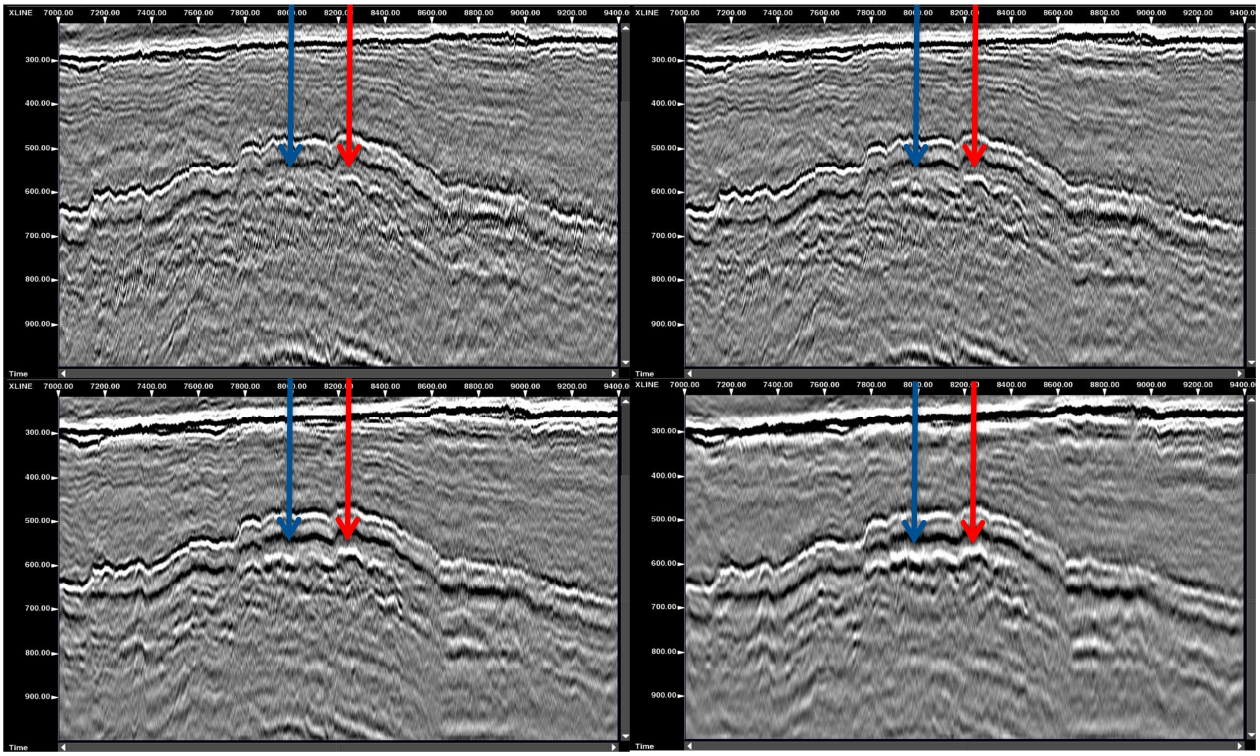

Figure 6: Angle-stacks from sea-surface reflection imaging. Top left: 0-10°. Top right: 10-20°. Bottom left: 20-30°. Bottom right: 30-40°. The area indicated by the red arrow exhibits a near to far slight, gradual increase in amplitude, while the area indicated by the blue arrow exhibits a much higher increase in amplitude from near to far angles.

DOI http://dx.doi.org/10.1190/segam2015-5869968.1

EDITED REFERENCES

Note: This reference list is a copyedited version of the reference list submitted by the author. Reference lists for the 2015 SEG Technical Program Expanded Abstracts have been copyedited so that references provided with the online metadata for each paper will achieve a high degree of linking to cited sources that appear on the Web.

REFERENCES

Grogan, P., A.-M. Østvedt-Ghazi, G. B. Larssen, B. Fotland, K. Nyberg, S. Dahlgren, and T. Eidvin, 1999, Structural elements and petroleum geology of the Norwegian sector of the northern Barents Sea: Proceedings of the 5th Petroleum Geology Conference, 247–259, http://dx.doi.org/10.1144/0050247.

Lu, S., D. Whitmore, A. Valenciano, and N. Chemingui, 2014, Enhanced subsurface illumination from separated wavefield imaging: First Break, **32**, no. 11, 87–92.

Rønholt, G., H. A. Aronsen, T. Hellmann, and S. Johansen, 2008, Improved imaging of the Snøhvit field through integration of 4C OBC and dual-azimuth streamer seismic data: First Break, **26**, no. 12, 61–66.

Rønholt, G., Ø. Korsmo, S. Brown, A. Valenciano, D. Whitmore, N. Chemingui, S. Brandsberg-Dahl, V. Dirks, and J.-E. Lie, 2014, High-fidelity complete wavefield velocity model building and imaging in shallow water environments — A North Sea case study: First Break, **32**, no. 6, 127–131.

Rutherford, S. R., and R. H. Williams, 1989, Amplitude-versus-offset variations in gas sands: Geophysics, **54**, 680–688, http://dx.doi.org/10.1190/1.1442696.

Sherwood, J. W. C., K. Sherwood, H. Tieman, R. Mager, and C. Zhou, 2014, Efficient beam velocity model building with tomography designed to accept 3D residuals aligning depth offset gathers: 76th Conference & Exhibition, EAGE, Extended Abstracts, doi:10.3997/2214-4609.20141153.

Wapenaar, K., E. Slob, E. Snieder, and A. Curtis, 2010, Tutorial on seismic interferometry: Part 2 — Underlying theory and new advances: Geophysics, **75**, 75A211–75A227, http://dx.doi.org/10.1190/1.3463440.

Whitmore, N. D., A. A. Valenciano, W. Söllner, and S. Lu, 2010, Imaging of primaries and multiples using a dual-sensor towed streamer: 80th Annual International Meeting, SEG, Extended Abstracts, 3187–3192.